

Automatic Onset Detection of Rapid Eye Movements in REM Sleep EEG Data

Andres Soler* Ole Drange* Junya Furuki** Takashi Abe***
Marta Molinas*

* Norwegian University of Science and Technology, Department of Engineering Cybernetics, Trondheim, Norway (e-mail: andres.f.soler.guevara@ntnu.no).

** University of Tsukuba, Graduate School of Comprehensive Human Sciences, Tsukuba, Japan (e-mail: s2021362@s.tsukuba.ac.jp)

*** University of Tsukuba, International Institute for Integrative Sleep Medicine (WPI-IIIS), Tsukuba, Japan, (e-mail: abe.takashi.gp@u.tsukuba.ac.jp)

Abstract: Rapid eye movements (REM) during sleep is a descriptor of the REM sleep stage. Parameters associated with REM sleep, such as REM sleep numbers, REM density, REM latency, and pre-REM negativity have been associated with the functional role of REM sleep. The temporal properties of these parameters appear to play an essential role in REM sleep, so precise knowledge of these temporal properties, particularly REM onset, can help elucidate the temporal dynamics of neural activity related to REM sleep. However, manual detection of this event is a time-consuming and subjective process that can be facilitated by an automatic detection tool. We developed an automatic REM onset detection algorithm based on features describing rapid eye movements and compared the results obtained with human detection by a sleep expert.

Copyright © 2021 The Authors. This is an open access article under the CC BY-NC-ND license (<https://creativecommons.org/licenses/by-nc-nd/4.0/>)

Keywords: Rapid Eye Movement (REM), REM onset detection, Polysomnography, REM sleep, EEG Signal, EOG signal, Sleep scoring.

1. INTRODUCTION

The first description of eye movements associated with low-voltage EEG and simultaneous dreaming was made in 1953 by Aserinsky and Kleitman and it is a characteristic that defines the REM sleep stage (Gottesmann (2009)). Parameters associated to REM sleep, such as number of REM sleep, REM density (Smith and Lapp (1991)), REM latency (Anseau et al. (1985); Pace et al. (2018)), and pre-REM negativity (Abe et al. (2004, 2008a)) have been associated with the functional role of REM sleep. This functional role has been associated with brain plasticity and memory (Stickgold et al. (2000)), and emotional processing (Maquet et al. (1996)). Many studies have also suggested a link between behavioural dysfunctions such as depression, post-traumatic stress disorder and chronic sleep deprivation with alterations in the REM sleep pattern (Gillin et al. (1981); Lahmeyer et al. (1983); Mellman et al. (1997); Feinberg et al. (1987)). Of particular interest to this work, are the temporal properties of REM before and after the onset of REM, which have been linked to specific neural activation in the brain (Abe et al. (2008a,b, 2004)). These works, clearly point out the relevance of identifying the exact timing of the rapid eye movement onset, and how the neural paths around the time immediately before and after onset, can illuminate on the potential functional role of REM sleep. Despite more than 60 years since the discovery of REM, and the clear indications of the important role this sleep stage seem to play in the

emergence of psychopathologies, the specific mechanism linking these dysfunctions and alterations in REM sleep remains unclear, as research on this mechanism and its functional significance has not progressed sufficiently (Abe et al. (2008b)). We presume that this can partly be attributed to the long time and effort required for manually detecting REMs and REM onsets. Precise knowledge of the onset of REM can help elucidate temporal dynamics of the neural activity related to REM sleep and contribute with more insights into this mechanism. Research in this topic would highly benefit from the development of an automatic algorithm that can accurately detect the onset of rapid eye movements during REM sleep. This paper offers an automated alternative to the detection of this event during REM sleep. The algorithm is based on precise characterization of the magnitude of rapid eye movements occurring during REM sleep, first presented in (Takahashi and Atsumi (1997)), which are used as features for designing the search algorithm. The performance of this algorithm is first visually examined and validated by a sleep expert and based on this evaluation, specific performance indexes show that a *Precision* of 0.68 a *Recall* of 0.96, and an *F1 score* of 0.79 were attained by the proposed algorithm. This algorithm for automatic detection of the precise onset of eye movement could assist EEG brain imaging studies of REM sleep in elucidating the functional role of REM sleep by shedding light on the mechanism of neural path activation at the onset of REM. At the same time, this algorithm can be used for purposes such as automatic sleep

stage scoring, calculation of REM density, and numbers of REMS, etc. Examples of such applications are provided in this paper.

2. METHODS

2.1 Dataset

The data set was obtained from Polynomnography recordings in 8 participants. The recordings were carried out at the Human Sleep Lab of the International Institute of Integrative Sleep Medicine. The data consist of an electroencephalogram (EEG) recorded from 128 scalp sites using an electrode cap (ActiveTwo system, BIOSEMI), an electrooculogram (EOG) was recorded from three electrodes (lower, left and right of eyes) and sub-mental electromyograms (EMG) recorded from three electrodes. Figure 1a illustrates the positions of the horizontal EOG electrodes EOG-R and EOG-L, that were used for the onset detection.

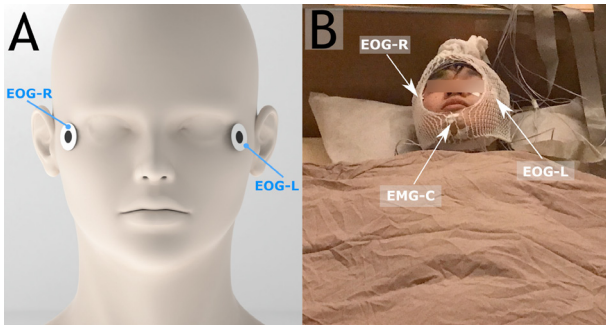


Fig. 1. (A) Positioning of the EOG electrodes on the left and right outer canthi. (B) Participant during PSG recording with EOGs and EMG-C electrode positions indicated

The recording period was approximately 8-hour of sleep for each participant, with a sampling frequency of 1024Hz. In this study, only the horizontal EOGs were used to detect the EM onset with the algorithm. A participant during the sleep PSG recordings is depicted in figure 1b. The study was approved by the Clinical Research Ethics Review Committee, University of Tsukuba Hospital (ID: R02-213). Written informed consent was obtained from each participant.

2.2 REM sleep scoring

The sleep stage scoring of the 8 participants was performed visually in continuous 30s epochs by sleep experts based on the criteria of the AASM (Berry et al. (2018)). The scoring for all participants resulted in 740.5 minutes of REM sleep in 1481 epochs. The algorithm was developed and optimized to detect the exact timing of the Eye Movement (EM) onset during the REM sleep portion of the data. The eye movements (EM) were defined according to the fulfillment of three basic criteria presented in Takahashi and Atsumi (1997). However, besides the pre-scored data, the algorithm has been tested on different sleep stages to investigate its potential as a sleep stage classifier by identifying REM sleep first. Running the algorithm on non-REM sleep is very different from REM sleep and should be further investigated as a sleep stage classifier.

2.3 Algorithm goal

The goal of the algorithm is to mark the onset of eye movements (EMs) in REM sleep. An example of EMs can be seen in figure 2 where the EM is marked with the dashed line. EMs are defined by sudden voltage deflections in the recordings of EOG-L and EOG-R channels suddenly spiking in opposite directions.

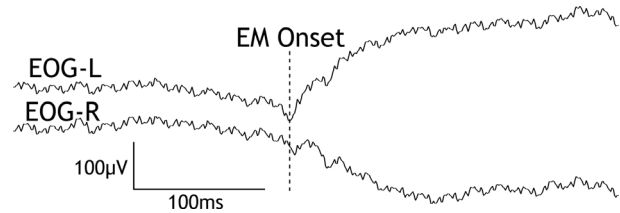


Fig. 2. Example of an EM spike, the dashed line indicates the EM onset in the raw data

2.4 Base algorithm

The detection of the EM in the base algorithm, originally reported in Takahashi and Atsumi (1997), is based on the definition of three basic REM-related EOG parameters: amplitude, duration, and slope of the EOG trace. The algorithm starts by pre-processing the data, re-sampling it to 80Hz, and smoothing it by applying a 7-point linear weighted moving average. Afterward, a double derivative is calculated to identify spikes such as seen in the figure 3. Where point A is the starting point of the slope and is found by the double derivative's first spike. Point B is the ending point of the slope and is a spike in point A's opposite direction. With all points A and B identified, the following three criteria are observed for the definition of EM onset:

- All points pairs (A and B) with an absolute value of point B minus point A higher than $30\mu V$ are accepted.
- The slope between the point pairs has to be higher than $248.3\mu V/s$.
- The slope duration has to be lower than 0.5s

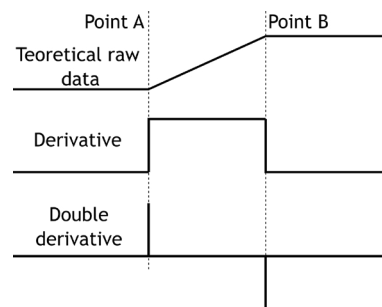


Fig. 3. Example of an idealized EOG signal, the derivative and double derivative of the signal. The points A and B correspond to the beginning and the end of the slope respectively. Notice that the ideal signal intends to show how the double derivative is useful to identify the two points

The points that fulfill the three criteria are then saved as EMs. An overview of the base algorithm is presented in figure 4.

Due to the presence of noise, the double derivative of the signals will lead to many unwanted spikes. Therefore, the base algorithm can mistakenly accept as EM points many of the spikes, leading to a large amount of unwanted confirmed EMs. A Low-pass filter was initially evaluated instead of the linear weighted moving average to attenuate the spikes, and a mixed technique with a low-pass filter and moving average were also tested. Despite these efforts, the results obtained with those approaches in the base algorithm were still ineffective in capturing the EM onsets correctly, and this was confirmed by visual inspection of the EMs detected. As a consequence of smoothing the signal with the low-pass filter, the spikes in the double derivative were misplaced compared to the raw signal. This misplacement leads to point A being marked close but not exactly on the actual EM starting point. The lack of efficacy in the results and the noise issues have led us to propose a new version of the algorithm to detect the EMs onset more accurately.

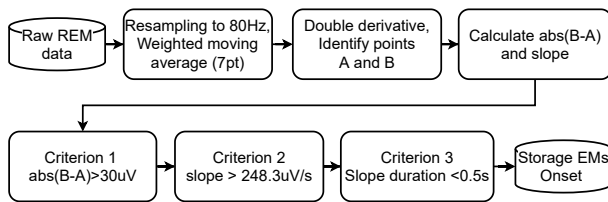


Fig. 4. Overview of Base Algorithm procedures according to Takahashi and Atsumi (1997)

2.5 Proposed algorithm

With the aim to improve the base algorithm efficacy in accurately identifying the EM onsets, more information from the shape and morphology of eye movements was incorporated into the proposed algorithm. The algorithm starts with subtracting signal EOG-R from EOG-L and then re-sampling the data to 300Hz. Afterward, it uses a linear weighted moving average with a 26-points to smooth the data. The linear weighted moving average limits the noise and gives better results than a low pass filter. After smoothing the signal, the derivative and double derivative are calculated. Notice that this version avoids the use of the double derivative to find the start and stop points of the EMs, instead, all the sample points are considered, and the double derivative is used to estimate the EM onset.

The first criterion to approve a sample as an EM point is that the change in the amplitude has to be greater than $80\mu\text{V}$ in less than 400ms. The second criterion is that the slope has to be higher than $500\mu\text{V/s}$ in the slope's starting point. The third criterion is that the average slope after the starting point has to be over $500\mu\text{V}$ for the following 125ms (37 samples). Then points that are approved by all three criteria are added to a list. These criteria are re-derived for this case from the individual EOG parameters and threshold values that constitute a well-defined REM-related EOG deflection according to Takahashi and Atsumi (1997). As the algorithm checks every point (300 per second), more than one point per actual EM might be accepted. As it is undesirable, the algorithm checks the gap between the approved EM points. For all EM points approved except the absolute first, it must have a 200ms gap from the last EM where the criteria are not met.

After the algorithm has identified only one EM point per actual EM, the position of the EMs is estimated by moving the points to a local maximum of the double derivative. The maximum movement of an EM point is 62ms forward or backward in time. In the next step, the algorithm checks for sudden deflections in the recordings of EOG-L and EOG-R channels in opposite directions. The slope from 21ms before the EM onset to 80ms after the EM onset is calculated for EOG-L and EOG-R channels. If the slope is more than $139\mu\text{V/s}$, the EM will be accepted by the algorithm. 21ms before the EM onset was chosen to avoid the influence of the negative spike the EMs has at the onsets. Some EMs have such a significant negative spike that the slope calculated from the EM onset to 80ms forward will give no slope. Moreover, checking 80ms after the onset is done to capture enough portion of the slope to identify the direction of deflection of the EOG channels, even if the channels spikes are unsynchronized. An example of these unsynchronized spikes can be seen in figure 2 where EOG-R moves upwards for about 20ms before moving down.

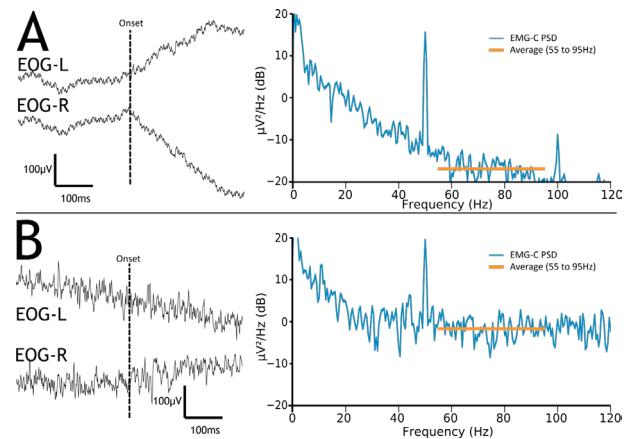


Fig. 5. EMs detected in (A) REM stage, (B) NREM stage, and their respective PSD from -5s to 5s from the onset.

Finally, to discriminate between EMs produced in REM sleep and the EMs miss-detected due to high EMG activity or at NREM stages, the algorithm calculates the power spectral density (PSD) of the EMG-c channel and the average PSD between 55 to 95Hz, then this value is compared with a threshold of -11dB, if the average is higher than -11dB the detected EMs was most likely from EMG high-frequency activity rather than actual REM. To explain this matter, figure 5 shows an example of two EOG windows, one in which the EMs detected by the algorithm agrees with the REM expert's scored windows 5a, and one in which the EMs detected by the algorithm does not agree with the REM scored windows 5b, the PSD of the signals are plotted at the right of the respective segment. From visual inspection of the PSD and its average between 55 to 95Hz on the right, it can be seen that the EMG activity has led to the detection of an EM in a NREM stage, and the PSD threshold can remove the miss-detected point from the EMs.

To attenuate the effects of the high noise and the lack of a low pass filter, the algorithm evaluated the criteria using the mean of 5 points instead of the specific point.

This eliminates some of the noise spikes that randomly get accepted by all the criteria. In 6 an overview of the proposed algorithm is presented.

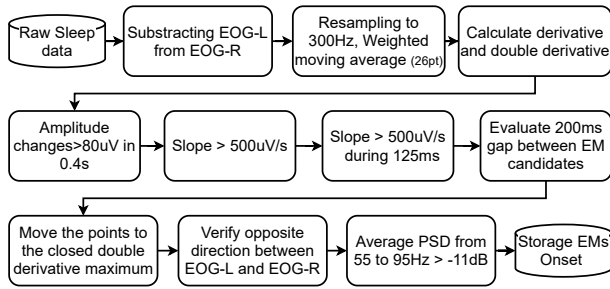


Fig. 6. Overview of the proposed algorithm

2.6 Comparison between the two algorithms

There are two important differences between the algorithms. The first is the method the algorithm uses to find points to check for the criteria. The base algorithm uses the double derivative to find the start and stop points, while the second checks the criteria on all points. This difference makes the base algorithm much faster but much more sensitive to noise. The base algorithm also tends to misplace some of the EM points. For example, if there is a noise spike before an EM, the base algorithm will set the noise spike and the actual EM spike as start and stop points respectively, and as the close points are removed afterward, the real EM onset will be removed. In contrast, the proposed algorithm will accept the same 2 points and remove the correct EM, but during the estimation of the EM position, it will move the noise point to the actual EM start.

The second difference is that the proposed algorithm evaluates the EOG-L and EOG-R channels individual spikes. This check makes sure that an EM is not triggered by only one of the channels spiking. A spike in one of the channels can be due to muscle movements which are considered noise. The algorithm also checks that the deflections after the spikes are in opposite directions. An opposite direction of the deflection is essential as the EM triggers the channels to move in opposite directions, while other movements such as heartbeat cause deflections in the same direction. Both these differences make the second algorithm slower but much more reliable, accurate and precise.

2.7 Algorithm performance

To evaluate the performance of the improved algorithm the following performance measures are used: precision, recall, and F1-score. Precision is the ratio of correctly predicted positive observations to the total predicted positive observations. In this case, how many of the positively rated EMs are correct. Recall or Sensitivity is the ratio of correctly predicted positive observations to the actual correct observations. In this case, how many of the actual positive EMs are rated positively. Combining these two parameters gives us the F1-score, which is the weighted average of Precision and Recall. Therefore, this score takes both false positives and false negatives into account and shows the overall performance. The parameters can be calculated by using the following equations:

$$\text{Precision} = \frac{\text{TruePositive}}{\text{TruePositive} + \text{FalsePositive}} \quad (1)$$

$$\text{Recall} = \frac{\text{TruePositive}}{\text{TruePositive} + \text{FalseNegative}} \quad (2)$$

$$\text{F1} = 2 * \frac{\text{Precision} * \text{Recall}}{\text{Precision} + \text{Recall}} \quad (3)$$

All three parameters are between 0 and 1, where 0 is the lowest performance, and 1 indicates perfect precision and recall. These parameters were selected because they do not consider the number of true negatives, then the bias from the number of possible points compared to the number of actual points is removed.

3. RESULTS

The performance of the proposed algorithm compared against the professionally marked EMs during REM sleep is presented in Table 1. Where P represents the participant number, TP true positive, FP false positive, and FN false negative. D is the average distance between professionally marked points and proposed algorithm points in the true positive cases. It is noticeable that in the mean F1 score a value of 0.79 was obtained, moreover, a mean recall value of 0.96 was achieved. It indicates that the algorithm detected 96% of the correct EMs with a mean distance of 6.7ms across participants.

P	TP	FP	FN	Recall	Precision	F1	D (ms)
1	44	10	6	0.88	0.81	0.85	7.5
2	389	97	4	0.99	0.80	0.89	5.0
3	361	151	3	0.99	0.71	0.82	6.4
4	481	154	1	1.0	0.76	0.86	7.3
5	107	168	4	0.96	0.39	0.55	8.5
6	595	162	12	0.98	0.79	0.87	5.3
7	168	115	4	0.98	0.59	0.74	5.4
8	518	367	40	0.93	0.59	0.72	8.5
Mean				0.96	0.68	0.79	6.7

Table 1. Algorithm Performance

The precision is relatively high with a value of 0.68, indicating that only 32% of the detected EMs were not considered by the professional scorer as EMs. The precision value was clearly attenuated by the large number of false positives obtained for some participants. E.g participant 5, the algorithm detected a larger number of false positives than true positives, however, 96% of the correct EMs were detected.

Visual inspection of the output of the algorithm shows to be promising. An average of 512 EM points (including false and true positives) from one of the participants is shown in figure 7b. Here a large negative spike in both the EOG channels can be observed. This negative spike is observed in previous works e.g. Abe et al. (2008b). After the negative spike, a positive overshoot with different amplitudes for the two channels is present. EOG-R does always have a higher overshoot after EM than EOG-left. If the EMs detected by the algorithm were very imprecise, the negative spike shown would be less sharp and with lower amplitude. Overall, the worse the EM detection accuracy is, the more flat the curve would appear. Figure 8a shows the algorithm EM detection when processing the whole night data, it shows that the detection appears to be reasonably good when compared to the REM stages

scored by a sleep expert, and 8b shows the improvement by adding the PSD criterion to remove EMs miss-detected due to EMG activity or during NREM stages. However, there are windows in which the algorithm does not detect actual EMs, especially when the EMs per window remain below 5. It can be seen from figure 8b, that these windows indeed are not in agreement with the sleep expert REM scored windows.

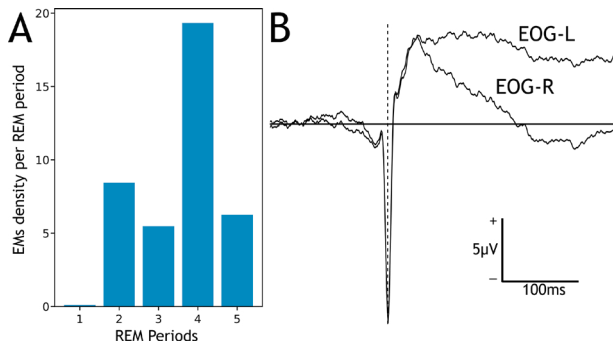


Fig. 7. (A) REM density (EMs in REM period / REM period length) in the REM periods over the night. (C) Average of EOG-R and EOG-L based on the EM points identified by the improved algorithm, average based on 515 EM points

To explain this matter, we use figure 5. In this figure, the effect of EMG artifacts can be seen in the portion of the raw EOG data, where muscle (EMG) and movement artifacts result from facial activity (Boukadoum and Ktonas (1986)). These artifacts, to affect the REM detection, might have had amplitudes higher than $30\mu V$. The frequency bandwidth of EMG activity is approximately 25 to 90 Hz and they are characterized by occurring in bursts. These features were verified in the windows that were not scored as REM by the sleep expert. The criterion of the PSD average between 55 to 95Hz can be employed to attenuate the influence of EMG signals on the EOG to values higher than the EM detection thresholds. The implementation of the PSD average has yielded the results observed in figure 8b.

4. DISCUSSION

Besides the main purpose of automatically identifying EM onsets during REM sleep, the algorithm developed in this paper has been tested for other possible applications which are discussed in the following:

4.1 Frequency of EM during REM periods

REM density measures the frequency of eye movements during REM sleep and in healthy participants, it increases over the course of the night and is highest when sleep pressure is lowest (Aserinsky (1969, 1973)). Previously reported works associate differences in EM frequency between healthy and depressive individuals (Goetz et al. (1996)), reduced EM density in Parkinson disease (Schroeder et al. (2016)), reduced EM density with aging (Darchia et al. (2003)), and increased EM density during learning (Smith et al. (2004)). In relation to these works, access to an easy tool that obtains EM frequency during REM sleep can prompt the use of EM frequency as a biomarker in such studies. In this study, the plot in fig 7a shows the changes in EM frequency across REM

periods during sleep for one of the participants. The EM frequency has increased from period 1 to 2, decreased in period 3, increased again in period 4 to decrease in the last period. This inverted pattern has been reported before in association with certain mental states (Kupfer (1978)).

4.2 Sleep stage scoring

The algorithm presented in this paper, which captures the REM onset, can be used for detecting REM sleep periods through the detection of the EM onsets. To achieve this, additional information from the EMG electrodes such as amplitude and frequency bandwidth were incorporated into the algorithm to account for the influence of EMG on the EOG data. This information is used to correct the fictitious EM detections done by the algorithm in epochs that are contaminated by EMG artifacts. With this EMG artifact detector, accurate scoring of REM according to the guidelines in AASM was possible. The result from this implementation is shown in figure 8b, where the REM scored windows are in very good agreement with the scores done by the algorithm. The advantage of using this algorithm for such purpose, compared to the Machine-Learning (ML) based classifiers reported in the literature, is the simplicity of the algorithm. The speed of detection of REM periods is about 10 min. While it does not offer the same speed as the machine learning based classifiers, it is much faster than the scoring done by a sleep expert using visual inspection. This algorithm can assist sleep experts in performing faster sleep staging. In contrast to the ML-based classifiers, it does not suffer from the problem of unbalanced REM sleep data (25% of REM sleep during the night), which affects the scoring accuracy of REM sleep (Yamabe et al. (2019)).

5. CONCLUSION

This paper designed and developed an algorithm for automatic detection of rapid eye movements onsets during REM sleep. The algorithm first developed a model of REM based on parameters and thresholds previously proposed on a heuristic basis and enhanced this model by incorporating additional morphological properties of the REM. The algorithm showed to be reasonably accurate in detecting EM onsets when compared to the onset labeled by a sleep expert. However, the heuristic or "customized" definition employed in this paper might not be sufficient to detect EM in data sets from other laboratories. Better characterization of REM parameters should be developed across wider populations to allow standardization of the detection process to enable comparative studies. Additional value of the algorithm is in its capability to extend its use as a sleep stage classifier through the detection of EM onsets. This proved to be feasible by the addition of an EMG artifact detector that could suppress the influence of EMG activity on the EOG recordings, and correctly detect actual EMs. The algorithm has also been shown to have practical value as an EM frequency counter, with potential use as a biomarker in clinical studies.

REFERENCES

- Abe, T., Matsuoka, T., Ogawa, K., Nittono, H., and Hori, T. (2008a). Gamma band EEG activity is enhanced after the occurrence of rapid eye movement during human REM sleep. *Sleep and Biological Rhythms*, 6(1), 26–33.

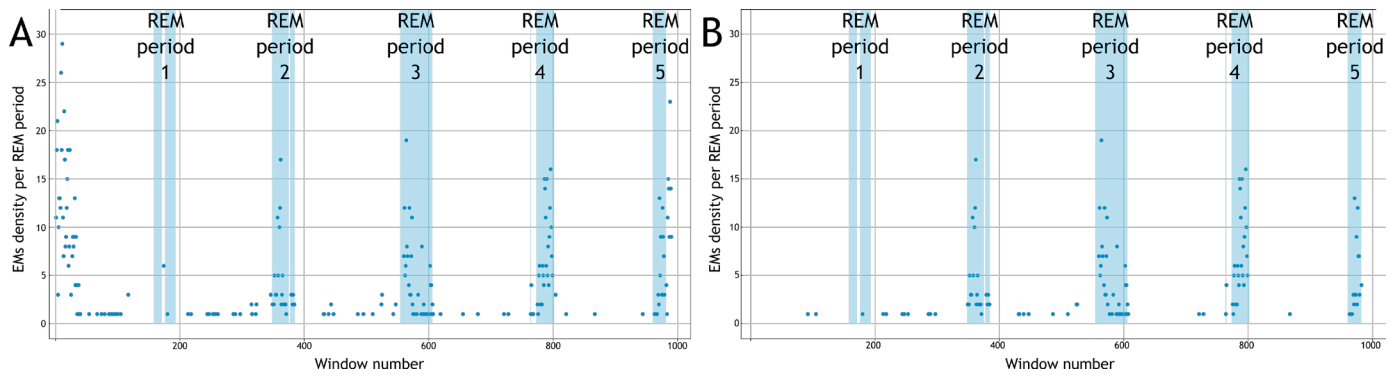


Fig. 8. (A) EMs per window compared to expert REM scored windows (shaded light blue) before applying the PSD criterion. (B) After applying the PSD criterion.

- Abe, T., Nittono, H., and Hori, T. (2004). Current sources of the brain potentials before rapid eye movements in human REM sleep. *International Congress Series*, 1270(C), 241–244.
- Abe, T., Ogawa, K., Nittono, H., and Hori, T. (2008b). Neural generators of brain potentials before rapid eye movements during human REM sleep: A study using sLORETA. *Clinical Neurophysiology*, 119(9), 2044–2053.
- Ansseau, M., Machowski, R., Franck, G., and Timsit-Berthier, M. (1985). REM sleep latency and contingent negative variation in endogenous depression suggestion for a common cholinergic mechanism. *Biological Psychiatry*, 20(12), 1303–1307.
- Aserinsky, E. (1969). The maximal capacity for sleep: rapid eye movement density as an index of sleep satiety. *Biological Psychiatry*, 1(2), 147–159.
- Aserinsky, E. (1973). Relationship of Rapid Eye Movement Density to the Prior Accumulation of Sleep and Wakefulness. *Psychophysiology*, 10(6), 545–558.
- Berry, R., Albertario, C., Harding, S., Lloyd, R., Plante, D., Quan, S., Troester, D., and Vaughn, B. (2018). ; for the American Academy of Sleep Medicine. *The AASM Manual for the Scoring of Sleep and Associated Events: Rules, Terminology and Technical Specifications*. American Academy of Sleep Medicine, Darien, LA, version 2.5 edition.
- Boukadoum, A.M. and Ktonas, P.Y. (1986). EOG-Based Recording and Automated Detection of Sleep Rapid Eye Movements: A Critical Review, and Some Recommendations. *Psychophysiology*, 23(5), 598–611. doi:10.1111/j.1469-8986.1986.tb00678.x.
- Darchia, N., Campbell, I.G., and Feinberg, I. (2003). Rapid Eye Movement Density is Reduced in the Normal Elderly. *Sleep*, 26(8), 973–977.
- Feinberg, I., Floyd, T.C., and March, J.D. (1987). Effects of sleep loss on delta (0.3-3 Hz) EEG and eye movement density: new observations and hypotheses. *Electroencephalography and Clinical Neurophysiology*, 67(3), 217–221.
- Gillin, J.C., Duncan, W.C., Murphy, D.L., Post, R.M., Wehr, T.A., Goodwin, F.K., Wyatt, R.J., and Bunney, W.E. (1981). Age-related changes in sleep in depressed and normal subjects. *Psychiatry Research*, 4(1), 73–78.
- Goetz, R.R., Wolk, S.I., Coplan, J.D., Weissman, M.M., Dahl, R.E., and Ryan, N.D. (1996). Rapid Eye Movement Density Among Adolescents With Major Depressive Disorder Revisited.
- Gottesmann, C. (2009). Discovery of the dreaming sleep stage: A recollection.
- Kupfer, D. (1978). Application of EEG Sleep for the Differential Diagnosis and Treatment of Affective Disorders. *Pharmacopsychiatry*, 11(01), 17–26.
- Lahmeyer, H.W., Poznanski, E.O., and Bellur, S.N. (1983). EEG sleep in depressed adolescents. *American Journal of Psychiatry*, 140(9), 1150–1153.
- Maquet, P., Peters, J.M., Aerts, J., Delfiore, G., Degueldre, C., Luxen, A., and Franck, G. (1996). Functional neuroanatomy of human rapid-eye-movement sleep and dreaming. *Nature*, 383(6596), 163–166.
- Mellman, T.A., Nolan, B., Hebding, J., Kulick-Bell, R., and Dominguez, R. (1997). A Polysomnographic Comparison of Veterans With Combat-Related PTSD, Depressed Men, and Non-Ill Controls. *Sleep*, 20(1), 46–51.
- Pace, M., Camilo, M.R., Seiler, A., Duss, S.B., Mathis, J., Manconi, M., and Bassetti, C.L. (2018). Rapid eye movements sleep as a predictor of functional outcome after stroke: a translational study. *Sleep*, 41(10), 1–11.
- Schroeder, L.A., Rufra, O., Sauvageot, N., Fays, F., Pieri, V., and Diederich, N.J. (2016). Reduced Rapid Eye Movement Density in Parkinson Disease: A Polysomnography-Based Case-Control Study. *Sleep*, 39(12), 2133–2139.
- Smith, C. and Lapp, L. (1991). Increases in Number of REMS and REM Density in Humans following an Intensive Learning Period. *Sleep*, 14(4), 325–330.
- Smith, C.T., Nixon, M.R., and Nader, R.S. (2004). Post-training increases in REM sleep intensity implicate REM sleep in memory processing and provide a biological marker of learning potential. *Learning and Memory*, 11(6), 714–719.
- Stickgold, R., Whidbee, D., Schirmer, B., Patel, V., and Hobson, J.A. (2000). Visual discrimination task improvement: A multi-step process occurring during sleep. *Journal of Cognitive Neuroscience*, 12(2), 246–254.
- Takahashi, K. and Atsumi, Y. (1997). Precise Measurement of Individual Rapid Eye Movements in REM Sleep of Humans. *Sleep*, 20(9), 743–752.
- Yamabe, M., Horie, K., Shiokawa, H., Funato, H., Yanagisawa, M., and Kitagawa, H. (2019). MC-SleepNet: Large-scale Sleep Stage Scoring in Mice by Deep Neural Networks. *Scientific Reports*, 9(1), 1–12.